Journal of Applied Mechanics and Technical Physics, Vol. 50, No. 5, pp. 809–818, 2009

NONSTATIONARY FORMATION OF NANODISPERSED COMPOSITES DURING VACUUM DEPOSITION OF A TWO-COMPONENT VAPOR

A. A. Bochkarev and V. I. Polyakova

UDC 699.017.23:536.423.1:621.315.592

A model based on the Langmuir adsorption model and a program for numerical simulation of nucleation and condensation on a cooled substrate were developed to describe the nonstationary phenomena observed in experiments on the production of nanodispersed composites by vacuum deposition of a two-component vapor. Calculations performed for a mixture of silver and water vapor have shown that the nucleation processes of the condensed phases of the components mutually stimulate each other with silver nucleation playing a leading role. A number of unusual phenomena have been found: an increase in the relative rate of water vapor condensation with a decrease in its partial pressure; the absence of stationary condensation modes; the existence of a boundary regime that separates modes with increasing and decreasing silver concentration in the condensate; the formation of porous skeletons consisting of a condensate of one of the components filled with nanoparticles of the other component. The dispersion properties of the condensates for various condensation modes and the adhesion of the condensate to the substrate were determined.

Key words: *nanodispersed composites, numerical simulation of condensation.*

In the 1900s, an experimental technology was developed to produce various nanodispersed composites of a metal and an organic compound with unique properties by simultaneous vacuum deposition of two vapor components in a cryogenic condenser [1, 2]. Experiments on the production of nanodispersed composites highlighted two problems: 1) impossibility of sustaining a long stable process without manual control; 2) high metal concentration in the end product even in the case of a vapor mixture with a low metal vapor concentration compared to the vapor concentration of the organic compound [3]. As a continuation of research into the production of nanodispersed composites, we performed a mathematical modeling of the condensation of a two-component vapor on a cryogenic surface. Silver and water vapor condensation on a surface at a temperature of 223 K was modeled. The calculations revealed a number of new effects which may allow an explanation of the unusual phenomena observed in experiments and help develop a more advanced technology for producing composites.

Model of Molecular Processes on the Surface of an Ideal Substrate. In the modeling of molecular processes on the surface of an ideal substrate, we used the simple phenomenological model described in [4]. This model consists of the following. Vapor condensation on a substrate in a vacuum chamber occurs through the adsorbed phase consisting of vapor molecules. The substrate surface is a homogeneous lattice of adsorption vacancies separated by a characteristic distance corresponding to the parameters of the crystal lattice of the vapor condensate. A vapor molecule reaching the surface of the crystal substrate is fixed in one of the adsorption vacancies with adsorption energy ε_s and is instantaneously equilibrated in temperature with the crystal surface. Due to thermal fluctuations and fluctuations of the vacancy-lattice vibrations, this molecule can move to a neighboring adsorption

Kutateladze Institute of Thermal Physics, Siberian Division, Russian Academy of Sciences, Novosibirsk 630090; anaboch@itp.nsc.ru. Translated from Prikladnaya Mekhanika i Tekhnicheskaya Fizika, Vol. 50, No. 5, pp. 95–106, September–October, 2009. Original article submitted July 11, 2008; revision submitted November 5, 2008.

vacancy, indicating surface diffusion, or it can be desorbed back into the vapor medium. The lifetime of a molecule before desorption is defined as

$$\tau_s \approx \nu^{-1} \exp\left(\varepsilon_s/(kT_s)\right).$$

Here $\nu \approx 10^{13}$–10^{14} is the frequency of thermal fluctuations of the adsorbed molecule, k is Boltzmann's constant, and T_s is the substrate temperature. For displacement of an adsorbed molecule to a neighboring vacancy, less intense fluctuations of thermal vibrations are required than for desorption; therefore, the lifetime of the molecule before displacement to a neighboring vacancy can be written as

$$\tau_{\rm SD} \approx \nu^{-1} \exp\left(\beta\varepsilon_s/(kT_s)\right),$$

where the subscript SD corresponds to surface diffusion and β is the contribution of the activation energy of surface diffusion U_d to the adsorption energy ε_s ($U_d = \beta\varepsilon_s$). The quantity β is determined by the geometry of the vacancy lattice. In [4], the value $\beta = 0.3$–0.4 is recommended. In the calculation of condensation, the value of β is refined by calculations for equilibrium states. The adsorption energy ε_s is calculated from the surface energy of the substrate or according to the Young hypothesis [5].

The probabilities of events (surface migration or desorption) are calculated as the reciprocal of the lifetime: $P_{\rm SD} \approx 1/\tau_{\rm SD}$, $P_s \approx 1/\tau_s$. During diffusion on the crystal surface, the adsorbed molecule can meet another molecule in a neighboring adsorption vacancy and or interact with it with bond energy ε_1. The quantity ε_1 can be calculated from the expression for the latent heat of evaporation taking into account the coordination number of the crystal lattice of the condensate (the number of the nearest neighbor atoms or molecules in the crystal with respect to the given atom). The lifetimes of each of two interacting molecules in neighboring adsorption vacancies before their diffusion or desorption are given by the expressions

$$\tau_{{\rm SD},i} \approx \nu^{-1} \exp\left(\beta(\varepsilon_{1,i} + \varepsilon_{s,i})/(kT_s)\right), \qquad \tau_{s,i} \approx \nu^{-1} \exp\left((\varepsilon_{1,i} + \varepsilon_{s,i})/(kT_s)\right.$$

(the subscript i denotes the component number).

Using the Model for a Two-Component Vapor. In the case of a two-component vapor, the model becomes complicated since the adsorbed molecule can have simultaneously several dissimilar neighbors in neighboring adsorption vacancies. Therefore, in calculating the lifetime of each molecule, it is necessary to take into account its interaction with the nearest neighbors with the corresponding bond energies. In the present work, it is assumed that the crystal lattices of the substrate and condensate are identical.

The model for surface molecular processes described here ignores the dynamics of intermolecular interaction and considers only the statistical behavior of surface molecules. Therefore, the goal of the present work is not to obtain quantitative results, but to describe some experimentally observed phenomena which are still poorly understood. The model is rather crude but simple, allowing a description of surface molecular processes with many involved molecules at considerable time intervals.

Adsorption Equilibrium. Due to desorption of previously adsorbed molecules, the flux of molecules leaving the substrate or condensate surface is given by

$$J_{s,i} = n_{M,i} \sum_{n_{M,i}} \frac{1}{\tau_{s,i}}. \tag{1}$$

Here the summation of the probabilities of desorption is performed for all $n_{M,i}$ molecules of the ith component with molecular weight M_i per unit surface area.

According to the molecular theory of gases, the flux of molecules through unit area of any section of a gas or vapor space is given by

$$J_{{\rm ch},i} = P_{{\rm ch},i}/(2\pi M_i k T_{\rm mix})^{1/2}. \tag{2}$$

Here $P_{{\rm ch},i}$ is the partial vapor pressure of the ith component in the chamber; M_i is the molecular weight of the ith vapor component; and T_{mix} is the temperature of the two-component vapor mixture.

The equilibrium state or the equilibrium concentration of the adsorbed vapor components on the substrate or crystal surface is given by the equality $J_{s,i} = J_{{\rm ch},i}$. The establishment of the equilibrium state of the adsorbate on the substrate or crystal surface is formally defined by the dynamic equation

$$\frac{dn_{M,i}}{dt} = J_{{\rm ch},i} - J_{s,i}, \tag{3}$$

whose physical meaning is the absolute rate of condensation.

From Eqs. (1) and (2), it follows that Eqs. (3) are equations of the relaxation type. Solutions of these equations at large computation times should give steady-state concentrations of the adsorbed vapor components on the substrate or condensate surface. Calculations using the model for the equilibrium state ($J_{s,i} = J_{\mathrm{ch},i}$) were used to refine the adsorption and bond energies and the contribution of the activation energy of surface diffusion.

Development of Vapor Condensation. According to classical nucleation theory, the adsorbed molecules collide due to surface diffusion, forming surface aggregates of molecules. At a certain degree of supersaturation, part of the aggregates become supercritical stable nuclei of the condensed phase, resulting in the formation of islets of the condensate on the crystal surface. Vapor molecules reaching the surface, migrate according to the surface diffusion mechanism, and are trapped in adsorption vacancies, where they are fixed by bonding to other molecules because their overall bond energy considerably reduces the probability of their migration and desorption. Nevertheless, desorption occurs. Some neighboring molecules are separated from each other to become single molecules and their desorption probability increases. However, this process is less effective than adsorption and condensation. The entire surface of the substrate is gradually filled with the condensate. New vapor molecules fall on the monolayer of molecules which are already fixed on the substrate. It is assumed that the monolayer of these molecules forms the same lattice of adsorption vacancies.

Equations (1) and (2) completely describe mass transfer between the vapor medium and substrate and can therefore be used to calculate the fraction of atoms or molecules remaining on the substrate. The relative condensation rate determined in such a manner is given by

$$\alpha_{c,i} = 1 - J_{s,i}/J_{\mathrm{ch},i}.$$

Algorithm for Numerical Computation. The proposed model of molecular processes of adsorption, nucleation, and condensation cannot be used to obtain an analytical solution. It is only suitable for numerical simulation of processes on the crystal surface. We developed a program for sequential simulation of the processes considered. The calculations are performed using a grid of adsorption vacancies (70×70) with a characteristic cell size equal to the crystal lattice constant. The characteristic time scale for modeling the events on the grid is set equal to the average time of arrival of vapor molecules at the grid which is minimal for two components. The cell at which a molecule arrives is not randomly chosen. In one time step, all cells are looked through sequentially. If the molecule is found in the examined cell, the following calculations are performed.

1. An analysis is made to determine in which molecular layer of this cell the surface molecule is present.

2. The nearest cells of the grid are analyzed. The total bond energy of the surface molecule in the examined cell is calculated depending on the filling of neighboring cells with molecules and taking into account the bonds with molecules in neighboring cells.

3. The activation energy of surface diffusion is calculated.

4. The probability of surface diffusion and desorption events of the surface molecule in the examined cell is calculated.

5. If the total probability of the indicated events is much lower than unity, the sum of the probabilities is normalized to unity.

6. Events are modeled using a random number generator. The random number generator is designed so as to reduce errors of the built-in computer generator.

7. If the desorption event is found, the surface molecule is removed from the examined cell.

8. If the molecule migration event is found, the random migration direction is modeled and the molecule is removed from the examined cell and added to a neighboring cell.

9. The lifetime of the molecule before the above-mentioned event is calculated. Then, this time is subtracted from the time step. The remaining time is used for repeated simulation for this cell beginning from Section 1 with the changed filling of this cell and the filling of neighboring cells taken into account.

10. When the time of analysis of the examined cell becomes equal to the time step, the next cell is analyzed.

After all cells have been analyzed, the arrival of the next molecule in a random cell is modeled. All current results are stored in a computer memory and then in output files. The current situation on the crystal surface is displayed on a monitor. When the number of molecules of the given sort that reach the surface becomes such that the total time of their arrival becomes equal to the time intervals of arrival of molecules of the other sort, the arrival of a dissimilar molecule at a random cell is modeled.

TABLE 1

Parameters for Calculation

Ag		H_2O	
Specified parameters			
Evaporator temperature, K	2000	Chamber temperature, K	300
Diameter of evaporator, m	0.12	Water vapor pressure, Pa	20–100
Substrate temperature, K	223	Lattice constant, m	$3.11 \cdot 10^{-10}$
Surface energy, N/m	0.8	Surface energy, N/m	0.074
Adsorption energy, J	$1.88 \cdot 10^{-19}$	Adsorption energy, J	$2.76 \cdot 10^{-20}$
Coadsorption energy, J	$1.88 \cdot 10^{-19}$	Coadsorption energy, J	$3.158 \cdot 10^{-20}$
Fraction of diffusion activation	0.46	Bond energy with silver, J	$2.0 \cdot 10^{-20}$
Calculated parameters			
Flux to substrate, $m^{-2} \cdot sec^{-1}$	$1.795 \cdot 10^{23}$	Flux to substrate, $m^{-2} \cdot sec^{-1}$	$(0.7–3.6) \cdot 10^{24}$
Flux from substrate, $m^{-2} \cdot sec^{-1}$	$-3.058 \cdot 10^{-13}$	Flux from substrate, $m^{-2} \cdot sec^{-1}$	$-1.623 \cdot 10^{23}$
Molecular volume, m^3	$1.716 \cdot 10^{-29}$	Molecular volume, m^3	$3.006 \cdot 10^{-29}$
Degree of supersaturation	$5.869 \cdot 10^{35}$	Degree of supersaturation	4.4–22.0
Crystal growth rate, Å/sec	$3.079 \cdot 10^4$	Time step, sec	$(0.6–3.0) \cdot 10^{-9}$
Arrival time		Time, μsec	0–353
of atoms to substrate, sec	$1.176 \cdot 10^{-8}$		

At the start of the program, fluxes of dissimilar molecules are supplied to the initially clean surface of the substrate crystal. The first vapor component is supplied from a thermal source. The flux of vapor molecules onto the substrate is calculated taking into account the geometry of the source and substrate and assuming spherical scattering of molecules from the source nozzle. The second component is supplied from a half-space filled with vapor at specified pressure and temperature. The dynamics of the number of component molecules in each layer on the condensation surface is calculated, and the total number of component molecules on the substrate is determined.

Calculation Results. The calculations were performed for a silver and water vapor mixture for the parameter values given in Table 1. The adsorption and coadsorption energies were calculated from the expression for the latent heat of evaporation of the condensate of the components and were then refined by testing the program for equilibrium conditions.

The calculations showed that dynamic equilibrium of the adsorbed molecules on the substrate was established in a time of about 10^{-6} sec. Subsequently, the number of water molecules adsorbed on the crystal surface continuously varied in time, remaining approximately equal to the average value. Local fluctuations of the number of molecules occur, leading to the formation of unstable aggregates of molecules in the adsorbed phase take place. These nuclei break down. Some nuclei of the condensed phase do not disappear but grow to take the shape of islets which gradually merge and fill the substrate. This is followed by nucleation of a condensed phase on the surface of the islets occurs, leading to an increase in their height. The process described above follows the classical scenario.

Figure 1 gives photographs of the condensate on the substrate obtained for five compositions of the vapor reaching the substrate (n is the number of water molecules). These compositions were calculated from the fluxes of the component molecules reaching the substrate. The upper row of photographs was obtained after 5000 water molecules had reached the substrate — the stage of nucleation of condensate islets. The arrangement of photographs from left to right corresponds to a decrease in the water vapor pressure in the chamber where condensation occurs. One can see an unusual phenomenon: a decrease in the pressure and degree of supersaturation of water vapor is accompanied by an increase in the number of islets of water condensate. Table 2 lists the parameter values corresponding to the photographs in Fig. 1. From Table 2 it follows that the number of water molecules attached to the substrate increases with decreasing degree of supersaturation, suggesting an increase in the relative rate of water condensation. This fact necessitates a more detailed analysis of the results. Table 3 gives the relative rates of silver and water condensation that correspond to the photographs in Fig. 1. From Table 3 it follows that as the water vapor pressure decreases by a factor of five, the relative condensation rate increases by a factor of five. In addition, a decrease in the water vapor pressure leads to a decrease in the relative rate of silver condensation. The observed phenomenon can be interpreted as the mutual stimulation of nucleation of the components. The existence of such a phenomenon was predicted in [6, 7].

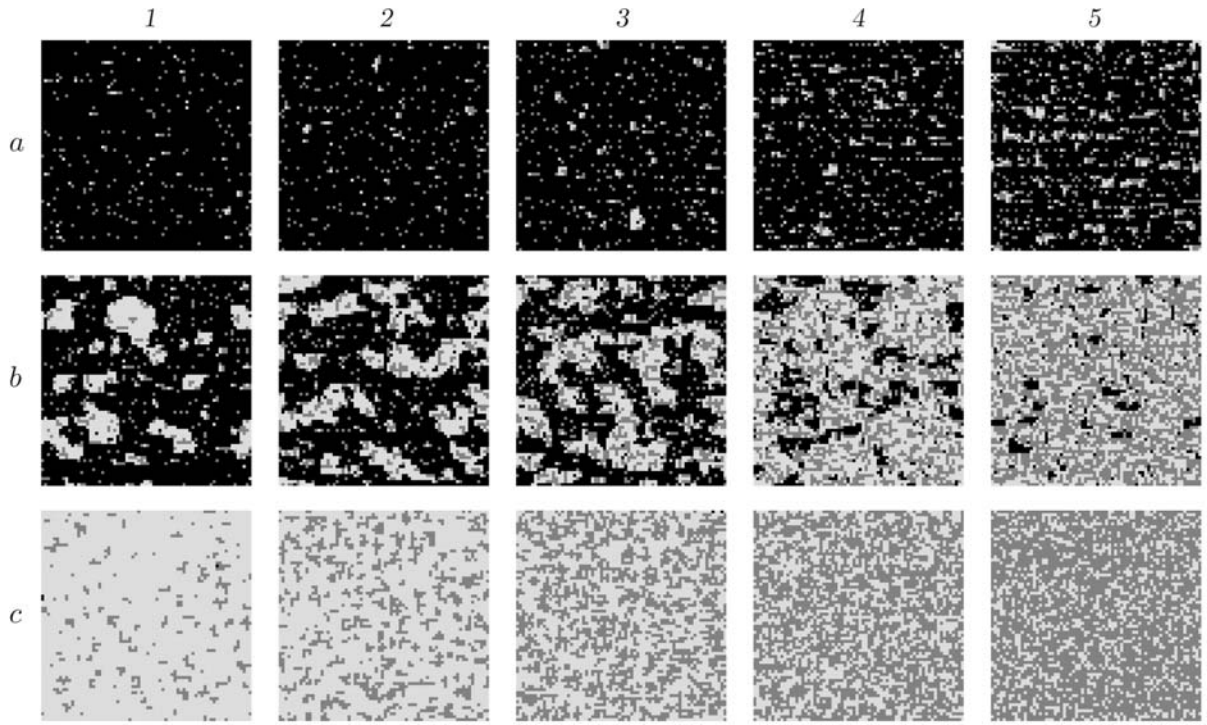

Fig. 1. Photographs of nanodispersed water–silver composite for n = 5000 (a), 20,000 (b), and 50,000 (c) and vapor compositions 5% Ag + 95% H_2O (1), 8% Ag + 92% H_2O (2), 10% Ag + 90% H_2O (3), 15% Ag + 85% H_2O (4), and 20% Ag + 80% H_2O (5); the black is the empty substrate, the light gray is the water condensate, and the dark gray is the silver condensate.

TABLE 2

Calculated Parameters and Calculation Results for Composites Shown in Photographs in Fig. 1

Vapor composition	Degree of H_2O vapor supersaturation	Number of H_2O molecules	Time, μsec	Number of Ag atoms reaching the substrate	Number of adsorbed Ag atoms	Number of adsorbed H_2O molecules
5% Ag + 95% H_2O	22.03	5000 20,000 50,000	2.955 11.801 29.530	251 1003 2509	217 527 1216	46 1220 13,654
8% Ag + 92% H_2O	15.42	5000 20,000 50,000	4.221 16.869 42.200	358 1434 3589	295 803 2015	61 1595 10,118
10% Ag + 90% H_2O	9.91	5000 20,000 50,000	6.563 26.220 65.560	558 2230 5576	428 1302 3471	129 2030 8793
15% Ag + 85% H_2O	6.61	5000 20,000 50,000	9.847 39.360 98.350	837 3347 8364	651 2344 5896	239 4060 9623
20% Ag + 80% H_2O	4.41	5000 20,000 50,000	14.815 59.010 147.530	1259 5018 12,548	956 3718 9289	461 4808 8968

TABLE 3

Relative Rates α_{Ag} and α_{H_2O} of Condensation for Composites Shown in Photographs in Fig. 1

H_2O vapor pressure, Pa	α_{Ag}			α_{H_2O}		
	$n = 5000$	$n = 20{,}000$	$n = 50{,}000$	$n = 5000$	$n = 20{,}000$	$n = 50{,}000$
100	0.865	0.525	0.485	0.009	0.061	0.273
70	0.824	0.560	0.561	0.012	0.080	0.202
45	0.767	0.584	0.622	0.026	0.102	0.176
30	0.746	0.700	0.705	0.048	0.203	0.192
20	0.759	0.741	0.740	0.092	0.240	0.179
Correlation coefficient						
1	0.969	−0.913	−0.987	−0.913	−0.893	0.882

The second row of photographs in Fig. 1 was obtained after 20,000 water molecules had reached the substrate — the stage of filling of the substrate. It is evident that, as the vapor pressure and degree of water supersaturation decrease, the amount of the water condensate and the relative rate of its condensation increase (see also row 6 in Table 3). However, the relative rate of silver condensation also increases. Apparently, in this stage, a decrease in the pressure and degree of supersaturation of water vapor leads to liberation of some adsorption vacancies for silver, resulting in an increase the relative rate of its condensation. In turn, the presence of silver stimulates water condensation by producing a greater number of growth steps.

The third row of photographs in Fig. 1 was obtained after 50,000 water molecules reached the substrate — the stage of developed condensation. From Table 3, it follows that, in this stage, as the pressure and degree of supersaturation of water vapor decreases, the relative rate of silver condensation increases and the relative rate of water condensation decreases. This is an expected result which is apparently due to a competition of dissimilar molecules at the same adsorption vacancies [8].

Table 3 gives correlation coefficients between the relative rates of silver and water condensation and the partial pressure of water vapor. The absolute values of the coefficients are close to unity, indicating their strong dependence on the partial water vapor pressure. The sign of the correlation coefficient corresponds to a direct or inverse correlation. From Table 3, it follows that, the stages of nucleation and substrate filling are accompanied by unusual phenomena: increasing the partial water vapor pressure leads to a decrease in the relative rate of water condensation, and in the nucleation stage, it leads to an increase in the relative rate of silver nucleation.

Calculations were also performed for identical times after the supply of vapor fluxes onto the substrate. The results show that, in the nucleation stage, the relative rate of silver condensation is high and the relative rate of water condensation is low. In all three stages, an increase in water vapor pressure leads to a decreases in the relative rate of silver condensation. This may be due to the fact that part of the adsorption vacancies occupied by water molecules are liberated for adsorption of silver atoms [8]. At the same time, in the stages of nucleation and substrate filling, an increase in water vapor pressure leads to a decrease in the relative rate of water condensation, indicating a significant dependence of the relative rate of water condensation on the relative rate of silver condensation. An acceptable correlation between silver and water condensation and water vapor pressure takes place only in the stage of developed condensation.

The detected difficult-to-explain phenomena appear to have a significant effect on the condensation process. Figure 2a shows variation in the condensate composition with time. The composition of the condensate was calculated from the sums of molecules of all condensate components. The peak in the initial region of the curves implies that condensation begins predominantly with silver nucleation. Then, the silver concentration in the condensate decreases sharply due to an increase in the relative rate of water condensation. The further dynamics of silver concentration in the composite varies widely with the composition of the vapor mixture reaching the substrate. An analysis of curves 1 and 2 obtained for $C_{Ag} = 5$ and 8%, respectively, shows that the silver concentration in the condensate decreases monotonically. An analysis of curves 3–5 shows that the silver concentration in the condensate, in contrast, increases monotonically. At a condensation time $t = 350$ μsec and $C_{Ag} = 5$, 8, 10, 15, and 20%, the silver concentration in the condensate are equal to 1.14, 9.44, 30.73, 47.58, and 58.94%, respectively. Thus, the silver concentrations in the vapor and in the condensate differ significantly.

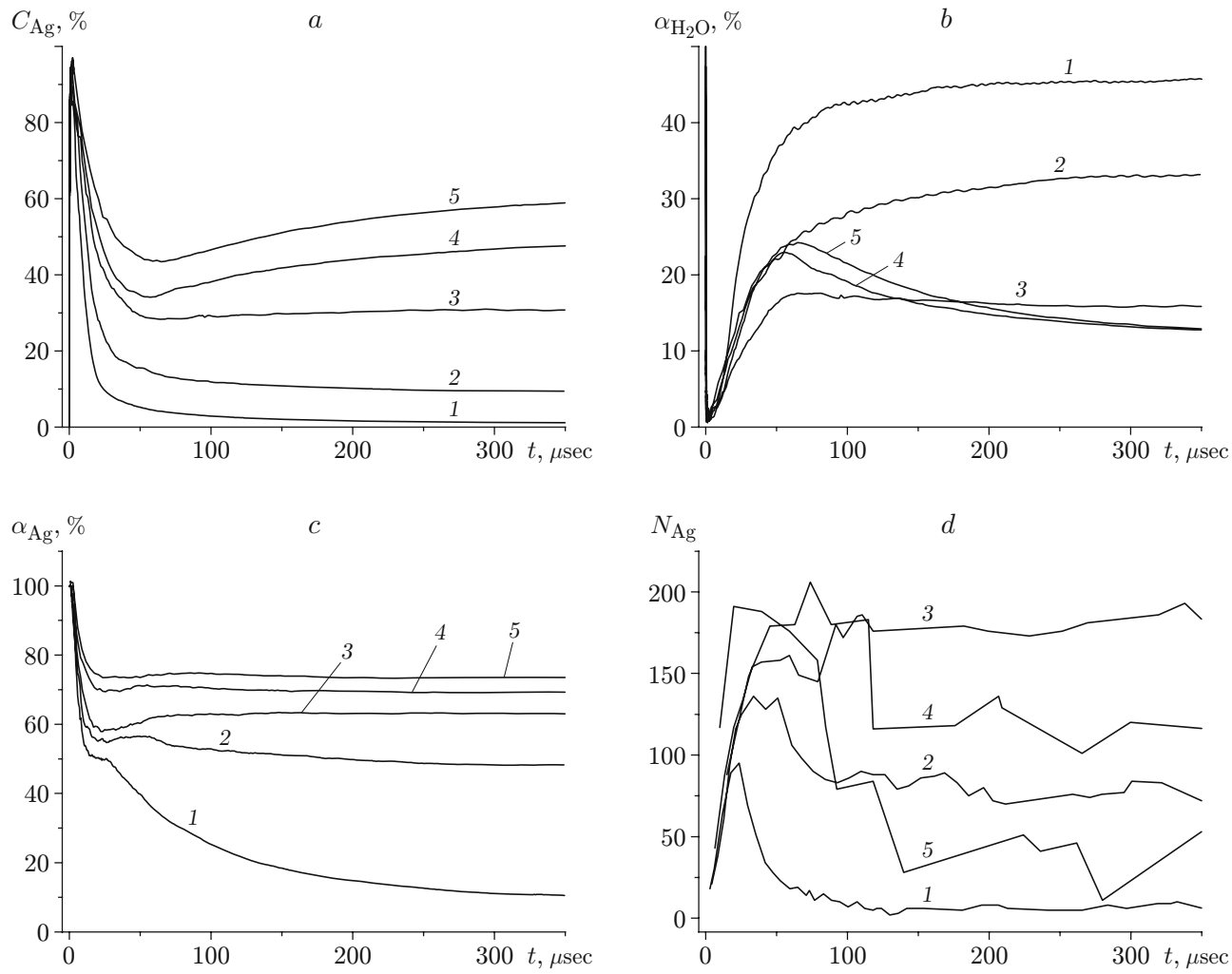

Fig. 2. Dynamics of silver concentration in the composite (a), relative condensation rate of water (b) and silver (c), and number of silver nanoparticles on the substrate (d) for various vapor compositions: 1) 5% Ag + 95% H_2O; 2) 8% Ag + 92% H_2O; 3) 10% Ag + 90% H_2O; 4) 15% Ag + 85% H_2O; 5) 20% Ag + 80% H_2O.

Figure 2b and c shows the dynamics of the relative rate of water and silver condensation. The high relative rates of condensation in the beginning of the process correspond to adsorption on free vacancies. The sharp reduction in the relative rate of silver condensation is caused by an increase in the degree of vacancy occupation, desorption and nucleation, and the blocking of the growth steps by the water adsorbate. The substrate is filled with the condensate at the times corresponding to the local minima in the curves presented in Fig. 2c. The characteristic breaks of the curves correspond to the onset of developed silver condensation. Subsequently, the relative rate of silver condensation on the condensate decreases at $C_{Ag} = 5$ and 8% (curves 1 and 2) and increases at $C_{Ag} = 10$, 15, and 20% (curves 3–5).

The dynamics of the relative rate of water vapor condensation (see Fig. 2b) differs significantly. The sharp decrease in the relative condensation rate at $t \approx 0$ is caused only by an increase in the desorption rate. The subsequent increase in the relative condensation rate is caused by an increase in the number of silver nuclei. After the substrate has been filled with the condensate, curves 1 and 2 ($C_{Ag} = 5$ and 8%) increase monotonically and curves 3–5 ($C_{Ag} = 10$, 15, and 20%) decrease monotonically. This difference in the dynamic curves of the relative condensation rate can be explained by a competition of the two vapor components during adsorption on the same vacancies. In [8, 9], this phenomenon was analyzed qualitatively; in the present work, it is confirmed by numerical calculations.

Size Distributions of Condensate Particles. The photographs of the substrate with the condensate were analyzed using the Texture 2 program to calculate the particle-size distribution of the condensate. The program allows one to record only particles on the substrate that are seen as continuous particles without foreign inclusions. The condensate in the form of a matrix on which foreign atoms or particles are visible is not recorded as a particle. Thus, the program provides full information on the particle-size distribution of the silver condensate at $C_{\mathrm{Ag}} = 5$, 8, and 10% and water at $C_{\mathrm{Ag}} = 15$ and 20%. In the remaining cases, the program allows one to record only separate particles. In view of this, the dynamics of the number of silver particles with cross section larger than one atom and the number of water particles can be analyzed using Fig. 2d. It is evident that, during nucleation, the number of silver particles increases rapidly for all examined values of C_{Ag}. At $C_{\mathrm{Ag}} = 5$ and 8%, the number of particles begins to decrease because part of the particles become coated with a water condensate. At $C_{\mathrm{Ag}} = 10\%$, this phenomenon is not observed; therefore, the number of particles continues to increase. At $C_{\mathrm{Ag}} = 15$ and 20%, the silver particles are united into a matrix and are not recorded by the program. In Fig. 2d, this shows up as a reduction in the number of particles, which is calculated with a large scatter.

Such an analysis of the particle-size distribution of water in the condensate indicates that the number of water particles increases rapidly during nucleation. Then, at $C_{\mathrm{Ag}} = 5$ and 8%, the number of the recorded water particles decreases due to the formation of a water condensate matrix. At $C_{\mathrm{Ag}} = 10\%$, there is also partial formation of the matrix from water ice. At $C_{\mathrm{Ag}} = 15$ and 20%, a stable number of water particles in the silver matrix is recorded by means of the program.

Discussion of Results. An analysis of the above results allows one to explain the unusual nature of condensation in experiments on the production of nanodispersed composites. From Fig. 2a, it follows that there is a limited number of modes in which condensation is approximately stable. It is impossible to predict these modes in experiments. If a mode is chosen inaccurately, there is a monotonic increase or decrease in the metal concentration in the composite. This circumstance leads to a need to continuously trace and adjust the mode in experiments. The results presented in Fig. 2a also explain why experiments with vapor containing a rather low metal vapor concentration yielded composites with high metal concentrations. The data obtained in the present work can be used to develop more reliable production technologies of nanodispersed composites.

From an analysis of the results in Fig. 2d, it becomes clear why in experiments it is difficult to produce a composite with metal particles of uniform size. An insignificant increase in the vapor metal concentration in the vapor mixture supplied to the substrate leads to the formation of a metal skeleton. After removal of the condensate from the condenser, this skeleton collapses to release metal particles. This fraction of metal particles can differ considerably from the particles produced by nucleation.

Additional processing of calculation results provides new important data. Calculations give the total number of silver atoms in each molecular layer of the condensate. These atoms belong to silver nanoparticles which have various shapes: from separate crystals oriented perpendicularly to the substrate to a highly porous metal skeleton. In addition, it is possible to calculate the polycrystal profile, which provides insight into the general growth process of metal crystals in the composite. From a physical point of view, the square root of the number of silver atoms in each molecular layer is an analog of the polycrystal radius R. The result of such a calculation is given in Fig. 3a (L_m is the number of molecular layers). It is evident that, for all examined silver concentrations in the vapor mixture supplied to the substrate, the polycrystal radius is smaller than the substrate size. During condensation at $C_{\mathrm{Ag}} = 5$ and 8%, the crystal radius first increases and then decreases in time, and the silver concentration decreases simultaneously. At $C_{\mathrm{Ag}} = 10$, 15, and 20%, the polycrystal radius stabilizes. As the silver concentration in the vapor mixture increases, the radius increases, always remaining smaller than the substrate size.

From Fig. 3a, it also follows that quasistationary condensation modes exist and the nonstationarity of modes (see Fig. 2a) is due to the strong nonstationarity in the stages of nucleation and substrate filling.

Figure 3b gives calculated silver atom concentrations in each molecular layer. In fact, these are silver concentration distributions across the condensate layer. In all cases considered, on the outer surface of the condensate there is a layer with an increased silver concentration. This implies that any new molecular layer is formed mainly by silver nucleation. In Fig. 3b, it is evident that, at $C_{\mathrm{Ag}} = 5$ and 8%, the molecular layers adjacent to the substrate have increased silver concentrations. The origin of these layers enriched in silver is difficult to explain. This may be a consequence of the fact that the silver nucleation process is more intense in the first molecular layer than in the other layers.

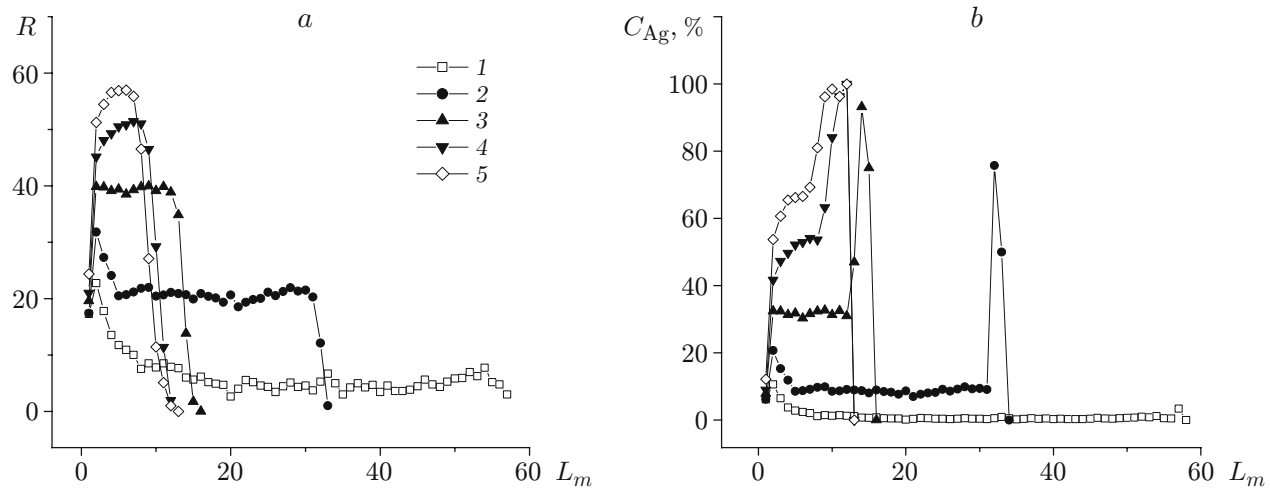

Fig. 3. Radius of the silver polycrystal in the composite (a) and silver concentration distribution over the height of the condensate layer (b) for various compositions of the vapor supplied to the substrate ($t = 352$ μsec): 1) 5% Ag + 95% H_2O; 2) 8% Ag + 92% H_2O; 3) 10% Ag + 90% H_2O; 4) 15% Ag + 85% H_2O; 5) 20% Ag + 80% H_2O.

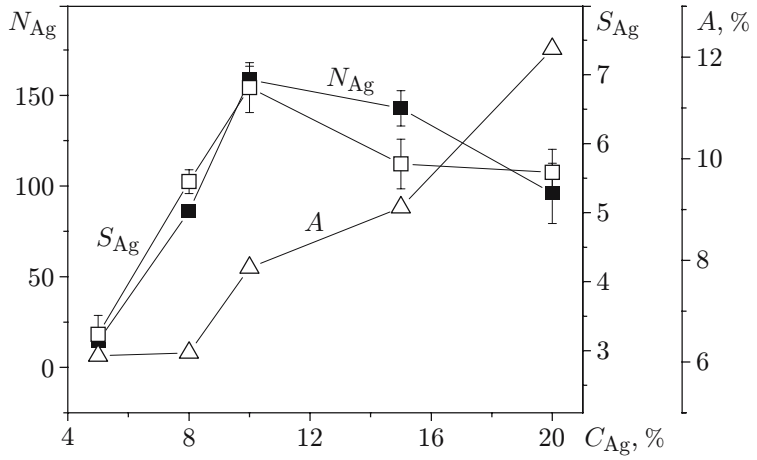

Fig. 4. Degree of adhesion A, the average number of nanoparticles N_{Ag}, and their average cross-sectional area S_{Ag} versus vapor silver concentration C_{Ag} in the starting mixture.

Using the calculation results, the adhesion of silver crystals to the substrate can be calculated as the fraction of the adsorption vacancies on the substrate occupied by silver atoms. Since, in the calculations, it is assumed that the energy of silver adsorption on the substrate is equal to the bond energy of silver atoms, the calculated adhesion is expressed in percentage of silver cohesion. The calculation results are given in Fig. 4. It is evident that, if the silver concentration in the deposited vapor mixture is insignificant, the silver adhesion to the substrate is insignificant. This facilitates the removal of the condensate from the substrate during production of a nanodispersed composite.

Figure 4 also gives the calculated average number and average cross-sectional area of silver nanoparticles. It is obvious that these quantities correlate with each other, i.e., as the numbers of particles in the condensate on the substrate increases, their size also increases. This information is useful in choosing the condensation mode for production of a composite with the required properties.

Conclusions. A model and a numerical simulation program for the nucleation and condensation of silver and water vapor mixture on a cooled substrate were developed using a modified Langmuir model adsorption. From the calculation results, it follows that, in the nucleation stage, there is mutual stimulation of the nucleation of condensed islets of the components. In the stage of developed condensation with the formation of a nanodispersed composite, silver nucleation plays a leading role in the formation of a new molecular layer.

Stationary condensation modes of the two-component vapor are absent. As the thickness of the condensed layer on the substrate increases, the integral composition of the nanodispersed condensate varies continuously. This is due to the fact that, in the stages of nucleation and filling of the substrate and at the onset of the developed condensation stage, the relative condensation rates of the components are greatly different and unstable. There the ratio of the vapor fluxes of the components supplied to the substrate has a critical value that separates the modes with monotonically increasing and decreasing silver concentration in the composite during condensation.

From the calculation results, it follows that condensation with a high silver vapor concentration leads to the formation of a metal skeleton filled with water ice particles, and condensation with a low silver concentration leads to the formation a skeleton of porous water ice containing silver particles. The results can be useful in choosing condensation modes for developing the production technology of nanodispersed composites with the required composition.

REFERENCES

1. A. A. Bochkarev and M. V. Pukhovoy, "Condensation of zinc and butanol vapors on a cryogenic surface," *J. Vacuum*, **48**, No 6, 579–584 (1997).
2. A. A. Bochkarev, M. V. Pukhovoy, and L. N. Kasyanova, "Kinetics of colloidal particle deposition on solid surfaces," *J. Colloid Interface Sci.*, **175**, 6–11 (1995).
3. A. A. Bochkarev, L. N. Kas'yanova, and M. V. Pukhovoy, "Hydrogen method for measuring dispersed-phase concentration in colloidal solutions of metals," *Zavod. Lab.*, No. 4, 34–35 (1994).
4. A. A. Chernov, E. I. Givargizov, Kh. S. Bagdasarov, L. N. Dem'yanets, V. A. Kuznetsov, and A. N. Lobachev, *Modern Crytsllogrpahy*, Vol. 3: *Formation of Crystals* [in Russian], Nauka, Moscow (1980).
5. V. Missol, *Surface Energy of Interfaces in Metals*, Slask, Katowice (1975).
6. A. A. Bochkarev and V. I. Polyakova, "Chain mechanism of heterogeneous nucleation in the presence of impurity," in: *Abstracts 2nd All-Union Conf. Modeling of Crystals Growth* (Riga, November 2–5, 1987), Stuchka Latvian State University, Riga (1987), pp. 84–86.
7. A. A. Bochkarev and V. I. Polyakova, "Features of the initial stage of condensation on a solid surface related to the migration of impurity," in: *Thermal-Physics Processes during Crystallization* (collected scientific papers) [in Russian], Institute of Thermal Physics, Novosibirsk (1987), p. 128–135.
8. A. A. Bochkarev, V. I. Polyakova, and Yu. G. Shukhov, "Influence of adsorption of residual atmosphere on heterogeneous condensation of metal vapor," in: *Thermal Physics of Crystallization and High-Temperature Treatment of Materials* (collected scientific papers) [in Russian], Institute of Thermal Physics, Novosibirsk (1990), pp. 98–117.
9. G. Held, M. Mayan, W. Sklarek and H.-P. Steinruck, "The influence of water on the formation of thin Cu films on Ni (111)," in: *Abstracts 14th Int. Vacuum Congress* (Birmingham, UK, August 31–September 4, 1998), S. n., Birmingham (1998), pp. 253–254.